NASA Technical Memorandum 88903

A General Method for Unsteady Stagnation Region Heat Transfer and Results for Model Turbine Flows

Tuncer Cebeci
California State University
Long Beach, California

Andreas Krainer
Naval Postgraduate School
Monterey, California

Robert J. Simoneau
Lewis Research Center
Cleveland, Ohio

Max F. Platzer
Naval Postgraduate School
Monterey, California

Prepared for the
2nd Thermal Engineering Conference
cosponsored by the ASME and JSME
Honolulu, Hawaii, March 22–27, 1987

A GENERAL METHOD FOR UNSTEADY STAGNATION REGION HEAT TRANSFER AND RESULTS FOR MODEL TURBINE FLOWS

Tuncer Cebeci
Center for Aerodynamics Research
California State University
Long Beach, California

Andreas Krainer
Naval Postgraduate School
Department of Aeronautics
Monterey, California

Robert J. Simoneau
National Aeronautics and Space Administration
Lewis Research Center
Cleveland, Ohio 44135

Max F. Platzer
Naval Postgraduate School
Department of Aeronautics
Monterey, California

ABSTRACT

Recent experiments suggest that the heat-transfer characteristics of stator blades are influenced by the frequency of passing of upstream rotor blades. The calculation of these effects requires that the movement of the stagnation point with variations in freestream velocity is properly represented together with the possible effects of turbulence characteristics on the thin leading-edge boundary layer. A procedure to permit the achievement of these purposes is described for laminar flows in this paper together with results of its application to two model problems which demonstrate its abilities and quantify the influence of wake characteristics on fluid-dynamic and heat-transfer properties of the flow and their effects on surface heat transfer.

NOMENCLATURE

a,b	= ellipse axes
D	= cylinder diameter
F	= blade passing frequency, $1/(t_g + t_w)$
f	= stream function, $\psi/(u_o L\nu)^{1/2}$
G	= nondimensional temperature, $(T_w - T)/(T_w - T_e)$
k	= thermal conductivity
L	= reference length
m	= $(T_w - T_e)^{-1}\,[d(T_w - T_e)/d\xi]$
Pr	= Prandtl number
$\dot{q}_w$	= wall heat flux
R_L	= Reynolds number, $u_o L/\nu$
St	= Strouhal number, FD/u_∞
T	= static temperature
t	= time
u,v	= boundary-layer velocity components
$\bar{u}_e$	= $u_e/[u_\infty(1 + \gamma)]$
u_o	= reference velocity, equal to $u_\infty(1 + \gamma)$ and u_∞ for first and second model problems, respectively
u_∞	= freestream velocity
w	= u_e/u_∞
x,y	= boundary-layer coordinates
$\bar{x},\bar{y}$	= Cartesian coordinates
z,z_o	= ϕ/γ, α/γ
α	= angle of attack
γ	= thickness ratio = b/a
Δ^*	= dimensionless displacement thickness, (17b)
η	= $(u_o/\nu L)^{1/2} y$
ν	= kinematic viscosity
ξ	= x/L
ρ	= density
τ	= nondimensional time, tu_o/L
ϕ	= polar angle related to $\bar{x},\bar{y}$ coordinates
ψ	= stream function
ω	= frequency

Subscripts and Symbols

e	= boundary layer edge
s	= stagnation point
w	= wall or wake

primes denote differentiation with respect to η

INTRODUCTION

Periodic reviews of gas turbine heat transfer (1-3) suggest that progress is being made in measuring and analyzing the complex flows associated with steady-state heat transfer in gas turbines. However, research on unsteady heat transfer in turbine passages is just beginning to appear. It is premature to evaluate the effects of wake-generated unsteady heat transfer on turbine durability but the research data to provide the necessary thermomechanical loads (4-13) are emerging rapidly. Dring, et al. (4) explored the nature of the boundary-layer response to turbine wakes and the unsteady pressure loading using thin-film surface sensors. Hodson (6) and Binder, et al. (7) mapped the convection of wakes through the rotor and flow properties in a rotor. Most of the heat-transfer data have been

obtained in short-duration facilities (8-11) or by using short duration techniques (12,13). Thin-film resistance thermometers provide information of surface temperature and are combined with a one-dimensional semi-infinite heat-conduction analysis to yield time-resolved heat flux. Dunn and coworkers have pioneered this technique and, in their most recent work (8,9), have begun to obtain time-resolved heat flux data in a real turbine stage at fully-scaled conditions. At the University of Oxford (10,11) rotor wakes are simulated with a spoked wheel rotating in front of a linear cascade. The results show that the wakes impinging on the airfoil can cause the local boundary layer to undergo transition and reverse transition at high frequency of the passing wakes. O'Brien et al. (12) used the transient technique in a steady-running rig, also with a spoked wheel wake generator, and showed excellent agreement between the time-average of the time-resolved heat transfer and more conventional steady-state data. Morehouse and Simoneau (13) in the same rig showed that it was necessary to separate the heat transfer effects due to the unsteady disturbances of periodic wakes from those generated by conventional turbulence.

In order to characterize the complex time-dependent flowfields, a number of promising approaches are being developed. Hodson (14) employed the two-dimensional inviscid code of Denton (15) and imposed a quasi-steady inlet boundary condition of a wake shape which moved across the inlet of the cascade at blade speed and calculated the movement of the wake as it passed through the cascade. Rai (16) has constructed a Navier-Stokes computer code with a complex arrangement of patched and overlaid grids and has attempted to reproduce the measurements of Dring (4) with some success.

An alternative approach which has proven reliable and very powerful in many external flows is to use interactive boundary-layer theory which requires the development of appropriate viscous and inviscid flow methods and their coupling by special techniques such as those described in (17-21).

As an essential preliminary to more extensive calculations involving complete blades, here we consider the development of an unsteady boundary-layer method for calculating the flow properties near the stagnation region of a blade where the movement of the stagnation point with space and time poses problems. We assume that the external velocity distribution is represented in dimensionless form by a function

$$u_e/u_\infty\,(x,t) = A(\xi,\tau)[\xi - B(\tau)] \qquad (1)$$

which allows the variation of the stagnation point and the freestream velocity. To evaluate the approach and the numerical procedure, we have chosen two model problems. The first one corresponds to flow over a thin ellipse in a constant freestream velocity field with a uniform wall temperature and with a local external velocity which changes with angle of attack. The second model problem considers flow over a circular cylinder again with a uniform wall temperature but with an external velocity distribution which allows changes in freestream velocity with time and simultaneous movement of the stagnation point caused by the change in position of a wake from a rotor blade.

The basic equations, initial and boundary conditions are considered in the following section and are followed by the results section. The paper ends with a summary of the more important conclusions.

BASIC EQUATIONS

For a two-dimensional, incompressible time-dependent laminar flow, the boundary-layer equations and their boundary conditions are well known, and for conditions with no mass transfer and specified wall temperature they can be written in the form:

$$\frac{\partial u}{\partial x} + \frac{\partial v}{\partial y} = 0 \qquad (2)$$

$$\frac{\partial u}{\partial t} + u\frac{\partial u}{\partial x} + v\frac{\partial u}{\partial y} = \frac{\partial u_e}{\partial t} + u_e\frac{\partial u_e}{\partial x} + \nu\frac{\partial^2 u}{\partial y^2} \qquad (3)$$

$$\frac{\partial T}{\partial t} + u\frac{\partial T}{\partial x} + v\frac{\partial T}{\partial y} = \frac{\nu}{Pr}\frac{\partial^2 T}{\partial y^2} \qquad (4)$$

$$y = 0, \quad u = v = 0, \quad T = T_w(x); \qquad (5a)$$

$$y = \delta, \quad u = u_e(x,t), \quad T = T_e \qquad (5b)$$

The determination of the initial conditions required for the above system is important and sometimes it can be arbitrary but in that event, the values of $\partial u/\partial t$ at $t = 0$ are nonzero; this implies an inviscid acceleration and, as a consequence, a slip velocity develops at the wall and is smoothed by an inner boundary layer initially of thickness $(\nu t)^{1/2}$ in which viscous forces are important. Thus a double structure develops in the boundary layer and may be treated by the numerical method described in (22). However, if interest is centered on the solution at large times, this feature may be reduced in importance by requiring that the initial velocity distribution satisfies the steady-state equation with the instantaneous external velocity. In addition, it is necessary to smooth out the external velocity $u_e(x,t)$ so that $\partial u_e/\partial t = 0$ at $t = 0$ and then standard numerical methods may be used and are stable. The use of a smoothing function makes for some loss of accuracy at small values of t but the error soon decays to zero once the required value of u_e is specified.

The calculation of upstream boundary conditions in the (t,y) plane at some $x = x_o$ when the conditions at a previous time line are known, can introduce different problems. To illustrate these difficulties for the case of a moving stagnation point, let us consider Eq. (1). Since $u_e = 0$ at the stagnation point by definition, its location based on the external streamlines is given by

$$\xi_s = B(\tau) \qquad (6)$$

Figure 1 shows the variation of the stagnation point with time according to the above equation with $B(\tau) = 1 + c\sin\omega\tau$, $c = 1$, $\omega = \pi/4$. We see that the stagnation point ξ_s is at 2 when $\tau = -2$ and at 0 when $\tau = 6$, etc. If ξ_s were fixed, we could assume that $u = 0$ at $\xi_s = -1$ for all time and for all y, but this is not the case. It is also possible to assume that the stagnation point is coincident with zero u-velocity for a prescribed time. However, we should note that the stagnation point given by Eq. (6) is based on vanishing external velocity. For a time-dependent flow, as we shall discuss later, this does not necessarily imply that the u-velocity is zero across the layer for a given ξ-location and specified time; flow reversals do occur due to the movement of the stagnation point and cause the locus of zero u-velocity to vary with ξ requiring the use of a special numerical method.

It is more convenient and useful to express Eqs. (2)-(5) in a form more suitable for computation. To

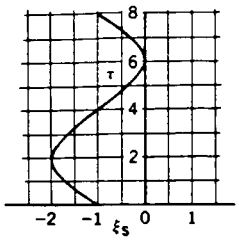

Figure 1. Variation of the stagnation point with time according to Eq. (1).

achieve this, we introduce the dimensionless variables τ, ξ, η, w, m, G together with a dimensionless stream function $f(\xi,\eta,\tau)$ and, with $\theta = \partial f/\partial\xi$, write Eqs. (2) to (5) as

$$f''' + f''\theta + \frac{\partial w}{\partial \tau} + w\frac{\partial w}{\partial \xi} = \frac{\partial f'}{\partial \tau} + f'\frac{\partial f'}{\partial \xi} \tag{7}$$

$$\frac{1}{Pr}G'' + G'\theta + m(1-G)f' = \frac{\partial G}{\partial \tau} + f'\frac{\partial G}{\partial \xi} \tag{8}$$

$$\eta = 0,\quad f = f' = G = 0;\quad \eta = \eta_e,\quad f' = w,\quad G = 1 \tag{9}$$

We use the Characteristic Box method to avoid the numerical problems associated with flow reversals in the stagnation region and to generate the initial conditions on the next time "line." This scheme requires that Eqs. (7) and (8) are expressed in terms of new coordinates. For this purpose, we note the definition of local streamlines and let $d\tau = d\xi/f'$. If the distance in this direction is designated by s and the angle that it makes with the τ-axis by β, (see Fig. 2) then the transformed momentum and energy equations (7) and (8) and their boundary conditions can be written as

$$f''' + f''\theta + \frac{\partial w}{\partial \tau} + w\frac{\partial w}{\partial \xi} = \lambda\frac{\partial f'}{\partial s} \tag{10}$$

$$\frac{1}{Pr}G'' + G'\theta + m(1-G)f' = \lambda\frac{\partial G}{\partial s} \tag{11}$$

$$\eta = 0,\quad \theta = f' = G = 0,\quad \eta = \eta_e,\quad f' = w,\quad G = 1 \tag{12}$$

where

$$\lambda = \sqrt{1 + (f')^2},\qquad \beta = \tan^{-1}f' \tag{13}$$

RESULTS AND DISCUSSION

The numerical solution of Eqs. (10) and (12) is obtained with Keller's Box method discussed, for example, in (23) for m = 0 (uniform wall temperature) and Pr = 0.72. In regions of no flow reversal, the Standard Box scheme was used. Where a calculation with this scheme revealed flow reversal, further iterations at that location made use of the Characteristic Box scheme described in (24-26) for two-dimensional unsteady flows and in (23,27) for three-dimensional steady flows. The application of the Characteristic method to the present problem, together with the procedure used to generate the upstream conditions is described in (28) and for this reason only the results are presented and discussed here for the two model problems. In all the calculations done here, the initial conditions were obtained by solving the steady-state form of the equations with the Standard Box scheme for uniform steplengths in ξ and in η. The stagnation point solutions were obtained from the similarity equations. A novel procedure based on the Characteristic Box scheme was used to compute the first solution on each time line with the initial calculations starting near the stagnation point based on the external velocity given by Eq. (1).

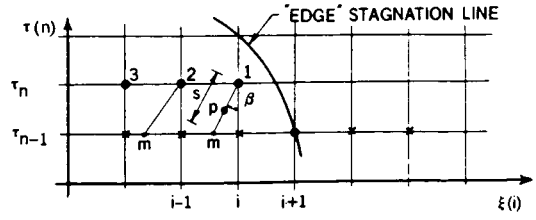

Figure 2. Notation and grid for the Characteristic Box scheme. For details, see (28).

Oscillating Airfoil Model

The first model problem corresponds to flow over an ellipse with a thickness ratio $\gamma(\equiv b/a)$ and with $\gamma \ll 1$ at an angle of α. The surface of the body is defined by

$$\bar{x} = -a\cos\phi,\quad \bar{y} = a\gamma\sin\phi,\quad -\pi < \phi < \pi \tag{14}$$

With these definitions and to a first-order approximation, the external velocity for the steady flow in the leading edge region of a thin ellipse can be deduced from inviscid flow theory to be

$$\bar{u}_e(z) = \frac{z + z_o}{\sqrt{1 + z^2}} \tag{15}$$

Here $\bar{u}_e(z)$ denotes a dimensionless velocity, the parameter z denotes a dimensionless distance related to the $\bar{x}$- and $\bar{y}$-coordinates of the ellipse by $\bar{x} + a = (1/2)a\gamma^2z^2$, $\bar{y} = a\gamma^2 z$ measured from the nose, and z_o represents a reduced angle of attack. The parameter z is also related to the dimensionless surface distance ξ with $L = \gamma^2 a$ by $\xi = \int_0^z (1 + z^2)^{1/2}dz$. In the present study we extend Eq. (15) to unsteady flows by introducing time dependency as

$$\bar{u}_e(z,\tau) = \frac{z + z_o(1 + c\sin\omega\tau)}{\sqrt{1 + z^2}} \tag{16}$$

Figures 3 to 5 show the calculated results for two circular frequencies, $\omega = \pi/30$, $\pi/3$ with $z_o = 1$ and $c = -1/2$. Figures 3 through 5 show the effects of the frequency on the wall shear f"(0), wall heat flux G'(0) and dimensionless displacement thickness, $\bar{\Delta}^*$, which are defined by

$$f''(0) = \frac{\tau_w}{\rho u_o^2}\sqrt{R_L},\qquad G'(0) = \frac{\dot{q}_w L}{k\sqrt{R_L}(T_w - T_e)} \tag{17a}$$

$$\bar{\Delta}^* = \frac{1}{L}\frac{u_e}{u_o}\sqrt{R_L}\int_0^\infty (1 - \frac{u}{u_e})dy \tag{17b}$$

The results of Figures 3a and 3b indicate that the time dependent effects on the solutions increase significantly as the circular frequency ω changes from $\omega = \pi/30$ to $\pi/3$. While the wall shear and displacement thickness values computed at $\omega\tau = \pi$ and 2π with $\omega = \pi/30$ are

nearly the same as those at $\tau = 0$, they differ considerably from each other when $\omega = \pi/3$. The results in Figure 4 show, however, that increasing the circular frequency by a factor of ten has practically no effect on the wall heat flux.

Figures 5 and 6 allow the examination of the effect the frequency has on the calculated velocity profiles in the vicinity of the stagnation point. Figure 5 shows

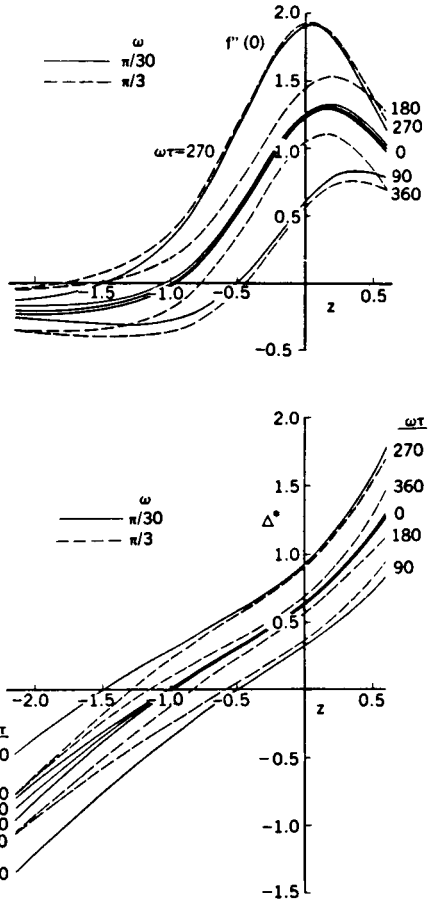

Figure 3. The effect of frequency on the (a) wall shear parameter, f"(0), (b) displacement thickness, Δ^*, of the first model problem.

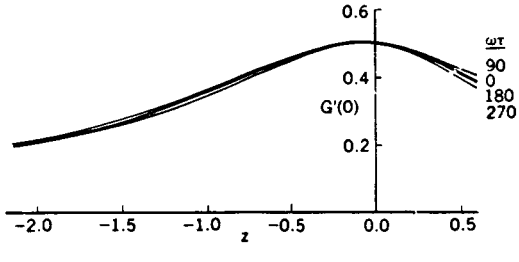

Figure 4. Variation of the wall heat flux parameter, G'(0), with z for the first model problem with $\omega = \pi/30$. The results with $\omega = \pi/3$ are virtually identical to those obtained with the smaller frequency.

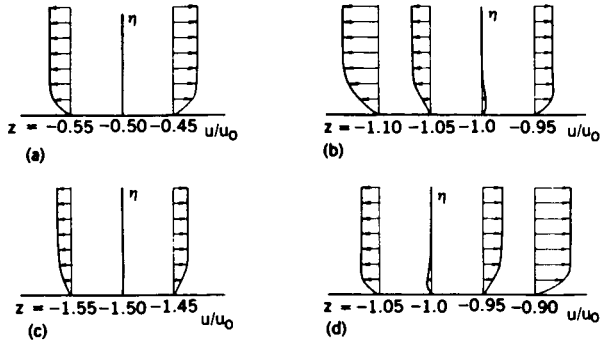

Figure 5. Variation of the velocity profiles for $\omega = \pi/30$ near the stagnation region of the first model problem for different values of $\omega\tau$, (a) 90, (b) 180, (c) 270, (d) 360.

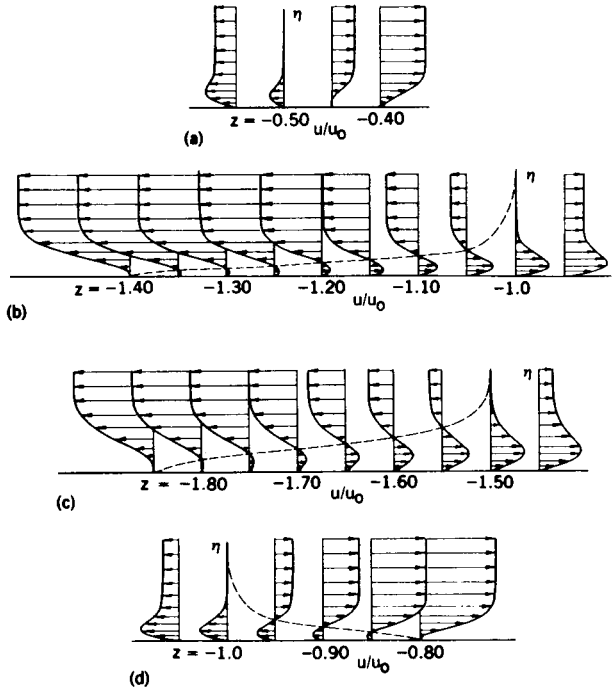

Figure 6. Variation of the velocity profiles for $\omega = \pi/3$ near the stagnation region of the first model problem for different values of $\omega\tau$, (a) 90, (b) 180, (c) 270, (d) 360. The dashed line indicates the locus of zero u-velocity.

that the locus of the u-velocity on time lines $\tau = \pi/2$ and π is essentially the same as in the steady case and as a result there are no flow reversals in the velocity profiles. However, as can be seen from Figure 6, increasing the frequency to $\pi/3$, flow reversals begin to occur around the stagnation point and become rather prolonged as time increases to $\omega\tau = 3\pi/2$. At $\omega\tau = 2\pi$, the region of flow reversal is reduced but is not zero, as it was at $\omega\tau = 0$.

Rotor Wake Model

The second model problem corresponds to a flow on a circular cylinder of diameter D, which experiences the periodic passing of the wakes from the turbine blades, see Fig. 7. For a time period t_g, the cylinder is subjected to a freestream velocity U_∞ and for t_w it is immersed in a superimposed moving wake which has a motion component u_b. The cycle repeats itself with a so-called blade passing frequency $F[\equiv 1/(t_g+t_w)]$ and is related to the Strouhal number St by FD/u_∞. We assume that the stagnation region of the cylinder is subjected to a velocity which varies in space and time according to Eq. (1), see (28), where

$$A(\tau) = \frac{[h^2 + 10(St)^2(1-h)^2]^{1/2}}{h} \tag{18}$$

$$B(\tau) = \tan^{-1}\left[3.3St\left(\frac{1}{h} - 1\right)\right] \tag{19}$$

$$h = \frac{1+u_m}{2} + \frac{1-u_m}{2}\cos[\pi(1 - 100\ St\tau)] \tag{20}$$

Here, u_m denotes the dimensionless minimum wake velocity.

Calculations are made for two values of Strouhal number taken equal to 0.1 and 0.2 with $u_m = 1/3$ in both cases. The computed values of wall heat flux, G'(0) show that they are not influenced by the changes in the freestream velocity and are virtually constant for the range of ξ and τ values considered with G'(0) ~ 0.50 for St = 0.1 and G'(0) ~ 0.51 for St = 0.2.

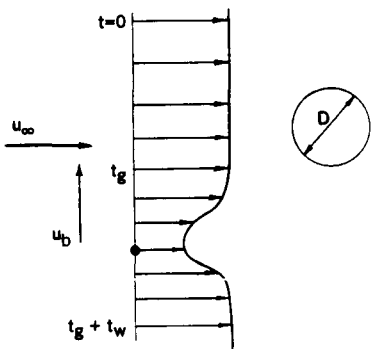

Figure 7. Notation and flow configuration for the second model problem.

On the other hand, as shown in Fig. 8, the computed values of wall shear, f"(0), for St = 0.1 are significantly influenced by the changes in the freestream velocity which causes flow reversals in the velocity profiles around the stagnation point based on the vanishing of the external velocity. The movement of the stagnation point and the resulting flow reversals increase with time and with space. For example, the calculations for steady state have the stagnation point at ξ = 0, and, as expected, there is no flow reversal in either side of the stagnation point. At τ = 0.05, the stagnation point moves to ξ = 0.15 but the flow reversals in the velocity profiles continue up to and including ξ = 0.85 as can be seen from the results shown in Fig. 9. At τ = 0.10, Fig. 9, the stagnation point has moved to ξ = 0.55 but the flow reversals persist for a longer distance and continue until ξ = 1.20. As can be seen from the velocity profiles in Fig. 9, the region of flow reversal across the layer has now increased and is substantially more pronounced than those at τ = 0.05.

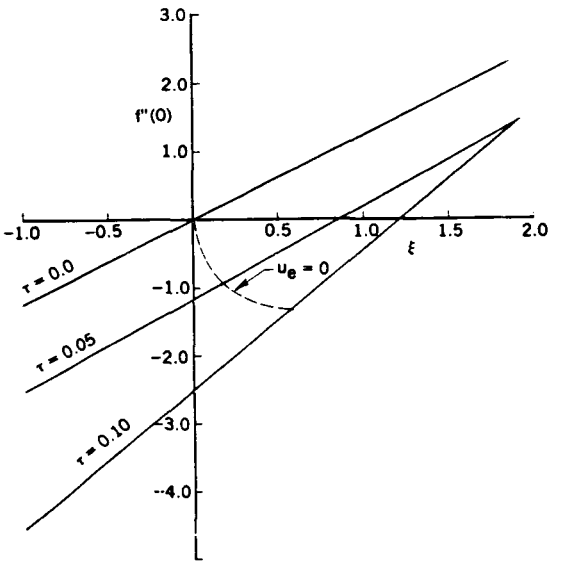

Figure 8. Variation of the wall shear parameter, f"(0), with ξ for the second model problem. St = 0.10.

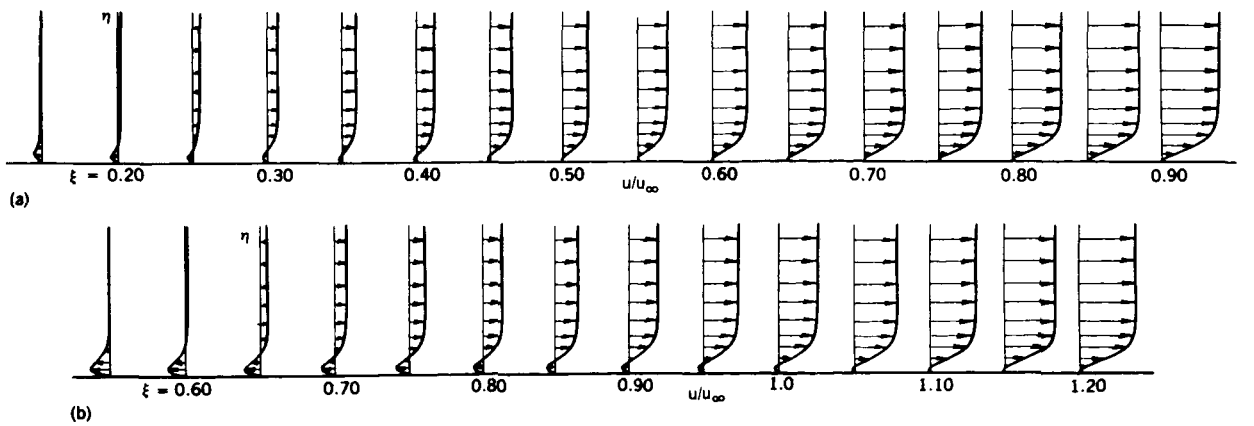

Figure 9. Variation of the velocity profiles near the stagnation region of the second model problem for two values of time. (a) τ = 0.05, (b) τ = 0.10.

The wall shear and displacement thickness results for St = 0.2 show similar trends. As expected, the flow reversals in the velocity profiles, for example at τ = 0.10, are bigger than those at St = 0.1 but cover the same range in ξ.

CONCLUDING REMARKS

A method for computing the heat transfer in the stagnation region of turbine blades is described for incompressible flows and evaluated for two model problems involving laminar flows. This method unlike the similarity methods of (29-31), however, is general and, with minor changes, can also be used for turbulent flows as well as for compressible flows.

The computed results show that the numerical procedure is able to obtain solutions for a range of blade-passing frequencies of practical relevance. The movement of the stagnation point with space and time and the resulting flow reversals around the stagnation point cause no computational difficulties and the numerical tests show that the accuracy is better than required for practical problems.

Acknowledgment: The research reported in this paper was conducted under NASA Lewis Research Center Grant, MIPR C-80017-F.

REFERENCES

1. Suo, M.: Turbine Cooling. In Aerothermodynamics of Aircraft Gas Turbine Engines (G.C. Oates, ed.), Chap. 19, AFAPL-TR-78-52, July 1978.

2. Metzger, D.E. and Mayle, R.E.: Heat Transfer: Gas Turbine Engines. Mech. Eng., Vol. 105, No. 6, pp. 44-52, 1983.

3. Simoneau, R.J.: Heat Transfer in Aeropropulsion Systems. In Heat Transfer in High Technology and Power Engineeering, (W.J. Yang and Y. Mari, ed.) pp. 285-319, Hemisphere Publishing Co., New York, 1987.

4. Dring, R.P, Joslyn, H.D., Hardin, L.W. and Wagner, J.H.: Turbine Rotor-Stator Interaction. J. Eng. for Power, Vol. 104, No. 4, pp. 729-742, 1982.

5. Sharma, O.P., Butler, T.L., Joslyn, H.D. and Dring, R.P.: An Experimental Investigation of the Three-Dimensional Unsteady Flow in an Axial Flow Turbine. AIAA Paper 83-1170, June 1983.

6. Hodson, H.P.: Measurements of Wake-Generated Unsteadiness in the Rotor Passages of Axial Flow Turbines. J. Eng. for Gas Turbines and Power, Vol. 7, No. 2, pp. 467-476, 1985.

7. Binder, A., Forster, W., Kruse, H. and Rogge, H.: An Experimental Investigation into the Effect of Wakes on the Unsteady Turbine Rotor FLow. J. Eng. for Gas Turbines and Power, Vol. 7, No. 2, pp. 458-466, 1985.

8. Dunn, M.G.: heat-flux Measurements for the Rotor of a Full-Stage Turbine: Part I, Time-Averaged Results. ASME Paper 86-GT-77, June 1986.

9. Dunn, M.G., George, W.K., Rae, W.J., Moller, J.C., Woodward, S.H. and Seymour, P.J.: Heat-Flux Measurements for the Rotor of a Full-Stage Turbine: Part II, Description of Analysis Technique and Typical Time Resolved Measurements. ASME Paper 86-GT-78, June 1986.

10. Doorly, D.J. and Oldfield, M.L.G.: Simulation of the Effects of Shock Wave Passing on a Turbine Rotor Blade. J. Eng. for Gas Turbines and Power, Vol. 107, No. 4, pp. 998-1006, Oct. 1985.

11. Ashworth, D.A., LaGraff, J.E., Schultz, D.L. and Grinrod, K.J.: Unsteady Aerodynamic and Heat Transfer Processes in a Transonic Turbine Stage. J. Eng. for Gas Turbines and Power, Vol. 107, No. 4, pp. 1011-1030, Oct. 1985.

12. O'Brien, J.E., Simoneau, R.J., LaGraff, J.E. and Morehouse, K.A.: Unsteady Heat Transfer and Direct Comparison to Steady-State Measurements in a Rotor-Wake Experiment. Heat Transfer 1986, Proceedings of the 8th Inter. Heat Transfer Conf., Vol. 3, pp. 1243-1248, Aug. 1986.

13. Morehouse, K.A. and Simoneau, R.J.: Effect of a Rotor Wake on the Local Heat Transfer on the Forward Half of a Circular Cylinder. Heat Transfer 1986, Proceedings of the 8th Inter. Heat Transfer Conf., Vol. 3, pp. 1249-1255, Aug. 1986.

14. Hodson, H.P.: An Inviscid Blade-to-Blade Prediction of a Wake-Generated Unsteady Flow. J. Eng. for Gas Turbines and Power, Vol. 107, No. 2, pp. 337-344, Apr. 1985.

15. Denton, J.D.: An Improved Time Marching Method for Turbomachinery Flow Calculation. ASME Paper 82-GT-239.

16. Rai, M.M.: Navier-Stokes Simulations of Rotor-Stator Interaction Using Patched and Overlaid Grids. AIAA Paper 85-1519, July 1985.

17. LeBalleur, J.C.: Couplage visqueux-non visquex: Methode Numerique et Applications Aux Ecoulements Bidimensionnels Transsoniques et Supersoniques. Le Recherche Aerospatiale No. 1978-2, 65, 1978.

18. Carter, J.E.: A New Boundary-Layer Inviscid Interaction Technique for Separated Flow. AIAA Paper 79-1450, 1979.

19. Veldman, A.E.P.: New Quasi-Simultaneous Method to Calculate Interacting Boundary Layers. AIAA J. 19, 769, 1981.

20. Cebeci, T., Stewartson, K. and Williams, P.G.: Separation and Reattachment Near the Leading Edge of a Thin Airfoil at Incidence. AGARD CP 291, Paper 20, 1981.

21. Cebeci, T., Clark, R.W., Chang, K.C., Halsey, N.D. and Lee, K.: Airfoils with Separation of the Resulting Wakes. J. Fluid Mech. 163, 323, 1986.

22. Cebeci, T., Stewartson, K. and Williams, P.G.: On the Response of a Stagnation Boundary Layer to a Change in the External Velocity. SIAM J. Appl. Math., Vol. 36, pp. 190-199, 1979.

23. Bradshaw, P., Cebeci, T. and Whitelaw, J.H.: Engineering Calculation Methods for Turbulent Flows. Academic Press, London, 1981.

24. Keller, H.B., Numerical Methods in Boundary-Layer Theory. Ann. Rev. Fluid Mech. Vol. 10, pp. 417-433, 1978.

25. Cebeci, T., Carr, L.W., Khattab, A.A. and Schimke, S.M.: Computational Aspects of Unsteady Flows. AGARD, CPP 386, France, May 1985.

26. Cebeci, T.: Unsteady Boundary Layers with an Intelligent Numerical Scheme. J. Fluid Mech. 163, 129, 1986.

27. Cebeci, T.: An Approach to Practical Aerodynamic Configurations. VKI Lecture Series on Computation of Three-Dimensional Boundary Layers Including Separation, 14-18 April 1986, Brussels.

28. Cebeci, T., Krainer, A., Platzer, M. and Simoneau, R.: A Numerical Procedure for the Flow and Heat Transfer Characteristics of the Stagnation Region of Stator Blades Subjected to Passing Wakes. NASA CR in preparation, 1986.

29. Ishigaki: Periodic Boundary Layer Near a Two-Dimensional Stagnation Point. J. Fluid Mech., Vol. 43, 1970, pp. 477-486.

30. Rott, N.: Unsteady Viscous Flow in the Vicinity of a Stagnation Point. Q. Appl. Math., Vol. 13, 1956, pp. 444-451.

31. Glauert, M.B.: The Laminar Boundary Layer on Oscillating Plates and Cylinders. J. Fluid Mech., Vol. 1, 1956, pp. 97-110.

1. Report No.	2. Government Accession No.	3. Recipient's Catalog No.
NASA TM-88903		

4. Title and Subtitle	5. Report Date
A General Method for Unsteady Stagnation Region Heat Transfer and Results for Model Turbine Flows	6. Performing Organization Code 553-13-00

7. Author(s)	8. Performing Organization Report No.
Tuncer Cebeci, Andreas Krainer, Robert J. Simoneau, and Max F. Platzer	E-3329
	10. Work Unit No.

9. Performing Organization Name and Address	11. Contract or Grant No.
National Aeronautics and Space Administration Lewis Research Center Cleveland, Ohio 44135	13. Type of Report and Period Covered Technical Memorandum
12. Sponsoring Agency Name and Address	14. Sponsoring Agency Code
National Aeronautics and Space Administration Washington, D.C. 20546	

15. Supplementary Notes

Prepared for the 2nd Thermal Engineering Conference, cosponsored by the ASME and JSME, Honolulu, Hawaii, March 22-27, 1987. Tuncer Cebeci, Center for Aerodynamics Research, California State University, Long Beach, California; Andreas Krainer and Max F. Platzer, Naval Postgraduate School, Department of Aeronautics, Monterey, California; Robert J. Simoneau, NASA Lewis Research Center.

16. Abstract

Recent experiments suggest that the heat-transfer characteristics of stator blades are influenced by the frequency of passing of upstream rotor blades. The calculation of these effects requires that the movement of the stagnation point with variations in freestream velocity is properly represented together with the possible effects of turbulence characteristics on the thin leading-edge boundary layer. A procedure to permit the achievement of these purposes is described for laminar flows in this paper together with results of its application to two model problems which demonstrate its abilities and quantify the influence of wake characteristics on fluid-dynamic and heat-transfer properties of the flow and their effects on surface heat transfer.

17. Key Words (Suggested by Author(s))	18. Distribution Statement
Heat transfer; Unsteady flow; Wakes; Boundary layer; Stagnation; Turbine	Unclassified - unlimited STAR Category 34

19. Security Classif. (of this report)	20. Security Classif. (of this page)	21. No. of pages	22. Price*
Unclassified	Unclassified		

*For sale by the National Technical Information Service, Springfield, Virginia 22161